An eco-friendly synthesis of 1,2-methylenedioxybenzene in vapour phase

A. Giugni[a], D. Impalà[a], O. Piccolo[b], A. Vaccari[a,*], A. Corma[c]

[a] Dipartimento di Chimica Industriale e dei Materiali, ALMA MATER STUDIORUM – Università di Bologna, Viale Risorgimento 4, 40136 Bologna, BO, Italy
[b] Studio di Consulenza Scientifica, Via Bornò 5, 23896 Sirtori, LC, Italy[1]
[c] Instituto de Tecnologia Quimica, Universidada Politecnica de Valencia, Avenida de los Naranjos s/n, 46022 Valencia, Spain

ARTICLE INFO

ABSTRACT

An environmentally friendly synthesis of 1,2-methylenedioxybenzene (MDB) was carried out, avoiding the use of any dihalomethane, reacting 1,2-dihydroxybenzene (DHB, also called catechol) with formaldehyde acetals in the vapour phase and in the presence of suitable heterogeneous catalysts. Ti-silicalite (TS-1) or some Ti-, Sn- or Zr-doped MCM-41 were extensively investigated for this role. Catalysts were characterised using different techniques, including BET surface area, X-ray diffraction, FT-IR spectroscopy and thermal gravimetric analysis. Some interesting results were obtained with either TS-1 or Sn-doped MCM-41, which shed light on the role of surface acidity, reaction temperature and residence time on the reactivity and catalyst deactivation. The subsequent regeneration of a spent catalyst was shown to be possible. Among the formaldehyde acetals investigated (dimethoxymethane, diethoxymethane, dipropoxymethane or 1,3-dioxolane), the results showed diethoxymethane to be the most suitable reagent, giving rise to selectivity values higher than 80% in MDB. Finally, a possible reaction pathway was proposed by indicating the role of 2-(ethoxymethoxy)phenol as a reaction intermediate and explaining the origin of observed by-products.

1. Introduction

The methylenedioxy-core is present in many active ingredients used in agrochemical and household products (for example piperonyl butoxide or PBO, an insecticide synergist), drugs (Tadafil[TM], Paroxetine[TM], etc.) or fragrances (Piperonal, Helional[TM]) [1–9]. Many of these products require intermediates prepared from 1,2-methylenedioxybenzene (MDB), so an economic and eco-friendly synthesis of the latter compound is fundamental.

Industrially, the synthesis of MDB is usually carried out in the liquid phase by reacting 1,2-dihydroxybenzene (DHB, also called catechol) with a dihalomethane (mainly dichloromethane) under alkaline conditions [10] while operating in a batch reactor. The reaction needs the presence of aprotic solvents such as dimethylsulfoxide [11,12], N-methylpyrrolidone [13] or dimethylformamide [14]. A process using a phase transfer catalyst was also reported [15]. Lastly, the KF-catalyzed methylenation of DHB was also studied, although only at the research level [16]. All these synthetic routes presented some relevant drawbacks, such as the use of potentially toxic solvents, the production of equimolar amounts of halogenated wastes, or an excess of inorganic salts, which may

be key factors as far as both environmental restrictions and the high cost of waste water treatment are concerned.

Although the gas phase alkylation of DHB has been widely investigated over the last few years [17–23], nowadays, there are very little published data on the one-step vapour phase synthesis of MDB [24,25]. Using Ti-silicalite (TS-1) as a catalyst and 1,3,5-trioxane (TOX) as source of formaldehyde [24], low-yield values were obtained by feeding a large molar excess of DHB if compared to the formylating agent (3:1), thus resulting in high recycling costs. On the other hand, using H-mordenite or AlF₃ as catalyst and, instead of TOX, a large excess of diethoxymethane (DEM) in comparison to DHB (10:1 as molar ratio) [25], MDB was obtained with high selectivity, but with very low yield values, due to both catalyst deactivation and decomposition of the alkylating agent. The aim of this study was to shed light on the key factors in the vapour phase synthesis of MDB from DHB and formaldehyde acetals (Fig. 1).

On the basis of published results, attention was initially focused on the TS-1 titanium silicalite for the study of reaction parameters. However, TS-1 presents micropores (5–6 Å) which are too small to allow DHB to enter them [26–31], so only part of the potentially active sites are actually available for the reagents. Therefore, after careful investigation of the role of the formaldehyde acetal as alkylating agent by using TS-1 as a catalyst, the focus was moved to the possibility of using doped MCM-41-type mesoporous catalysts to make the active sites inside the pores accessible to the reagents, thus affecting the selectivity of the reaction. As previously reported, doped MCM-41 molecular sieves are extremely active in alkylation

* Corresponding author. Tel.: +39 051 2093683; fax: +39 051 2093679.
E-mail address: angelo.vaccari@unibo.it (A. Vaccari).
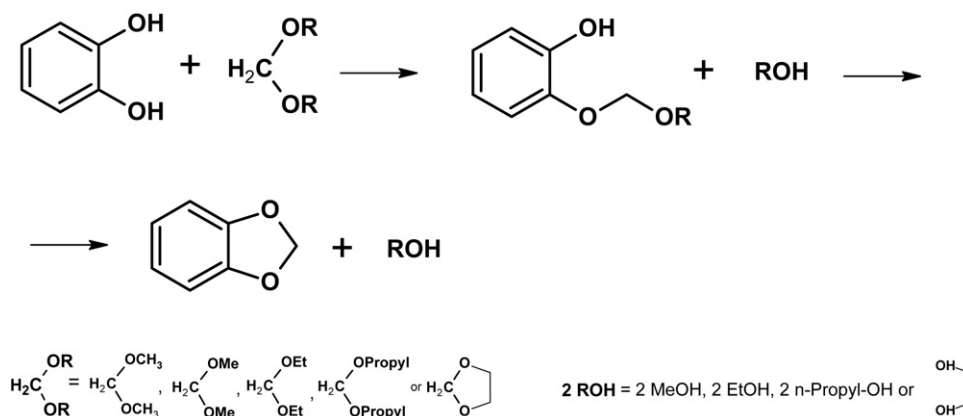[1] http://www.scsop.it.

Fig. 1. Reaction scheme between 1,2-dihydroxybenzene (DHB) and formaldehyde acetals to form 1,2-methylenedioxybenzene (MDB).

reactions, in either the liquid or the vapour phase [32–39], by offering the additional possibility of a reaction inside the larger pores of the mesoporous structure (20–40 Å). MCM-41 materials have channels in a hexagonal array, long-range order and surface areas up to 700 m^2 g^{-1} [40–42].

2. Experimental

2.1. Materials

1,2-Dihydroxybenzene (DHB, also called catechol), 1,2-methylenedioxybenzene (MDB), diethoxymethane (DEM), dimethoxymethane (DMM), 1,3-dioxolane (DOX), 1,3,5-trioxane (TOX), 3-methylcatechol (3-MC), Zr– and Ti–acetylacetonate (Zr–Ac and Ti–Ac), Ti(OEt)$_4$, SnCl$_4$·5H$_2$O, ZrOCl$_2$·8H$_2$O and Al(OH)$_3$ were purchased from Aldrich Chemicals (≥99.0 wt.%). Amorphous Aerosil 200 silica was purchased from Degussa, a 25 wt.% solution of tetramethylammonium hydroxide (TMAOH, K + Na < 5 ppm) was purchased from Alfa, hexadecyltrimethylammonium bromide powder (CTABr) was purchased from Merck (≥95.0 wt.%). The reagents were used without further purification. Hexadecyltrimethylammonium hydroxide (CTA-OH) was prepared by anion exchange of CTABr on an Amberlite-type resin (Aldrich), carried out at 303 K for 24 h with an Amberlite/CTABr molar ratio = 1.0. The process was repeated twice, so as to increase the exchange yield to 98.0%.

The synthesis of 2-(ethoxymethoxy)phenol (2-EMP) was carried out in the liquid phase under reflux at 353 K for 2 h, by using 4.0 g of DHB (0.036 mol), 11.0 g of DEM (0.106 mol) and 0.5 g of SiO$_2$ powder (Si-1803 by Engelhard, surface area = 300 m^2 g^{-1}, porosity = 0.5368 cm^3 g^{-1}). The reaction mixture was filtered, and ethanol and residual DEM were removed under a reduced pressure (<100 Pa). The synthesis of dipropoxymethane (DPM) was carried out in the liquid phase under reflux at 370 K by reacting an excess of n-propanol with DMM, operating with a molar ratio equal to 5.0 and using SiO$_2$ powder (Si-1803) as a catalyst. In order to shift the equilibrium towards the formation of DPM, methanol was continuously removed from the reaction mixture by means of Dean–Stark apparatus. The reaction mixture was filtered, and n-propanol and residual DMM were removed under reduced pressure (<100 Pa).

2.2. Catalyst preparation

The TS-1 (Si/Ti = 20 mol/mol) was prepared according to the literature [26–31]. Ti-, Zr- and Sn-containing MCM-41 samples were prepared using amorphous Aerosil 200 silica as an Si source, with a 25 wt.% aqueous 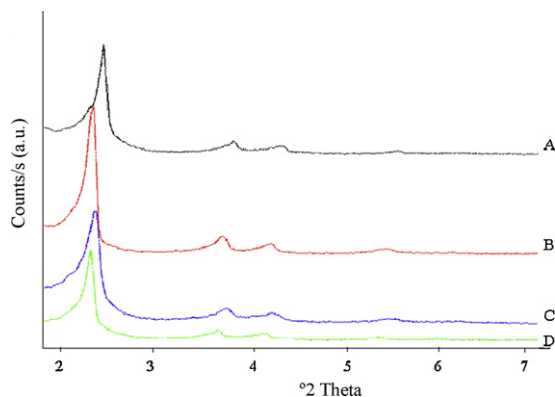solution of TMAOH and solid CTABr used as a mineralizer and template, respectively [41,43–48]. To obtain the Ti-containing samples, firstly a solution of CTABr and TMAOH in deionised water was prepared, and, when it was perfectly homogenized, the required amounts of Aerosil 200 SiO$_2$ and Ti(OEt)$_4$ were added. The resulting gel (I) (see below) was heated at 373 K for 48 h in a Teflon-lined stainless steel autoclave under static conditions. The procedure was the same for the synthesis of Zr-containing samples, using ZrOCl$_2$·8H$_2$O instead of the Ti(OEt)$_4$, and the resulting gel (II) (see below) was heated at 408 K for 24 h in the same autoclave cited above. The synthesis of Sn-containing samples was performed according to Ref. [46]: a solution of CTABr, CTA-OH and TMAOH in deionised water was prepared first, and when it was perfectly homogenized, Aerosil 200 SiO$_2$ and SnCl$_4$·5H$_2$O were added, and the resulting gel (III) (see below) was heated at 408 K for 24 h in the same autoclave as previously reported. The molar ratios of the gels subjected to hydrothermal treatment were:

I) SiO$_2$:0.15 CTABr:0.26 TMAOH:24.3 H$_2$O:x Ti(OEt)$_4$.
II) SiO$_2$:0.15 CTABr:0.26 TMAOH:(24.3 − 8x) H$_2$O:xZrOCl$_2$·8H$_2$O.
III) SiO$_2$:(0.15 − 4x) CTABr:4x CTA-OH:0.26 TMAOH:(24.3 − 5x) H$_2$O:x SnCl$_4$·5H$_2$O.

To prepare the Si-MCM-41 sample, the procedure was the same as that of the gel (I), with x = 0, i.e. omitting the addition of Ti(OEt)$_4$. Moreover, four samples doped with Al (in addition to Ti, Sn and Zr) were prepared using the synthesis previously reported for the Al-free samples, by adding the appropriate amount of Al(OH)$_3$. Finally, all the solid materials (prepared as previously reported), were filtered, washed with distilled H$_2$O, and dried in air at 333 K for 16 h. Then, the template was eliminated by heating the samples at 813 K under an N$_2$ flow of 150 mL min^{-1} for 1 h, followed by a calcination for 6 h under a flow of 150 mL min^{-1} at the same temperature.

2.3. Catalyst characterisation

X-ray diffraction (XRD) analyses were carried out using a Philips X'pert diffractometer, operating at 40 kV, 35 mA, and with a Cu Kα radiation (λ = 0.15118 nm). A 2θ range from 1° to 20° was investigated. BET surface area values were determined by the physical adsorption of N$_2$ at 77 K using a Micromeritics AUTOCHEM 2910, by pre-treating the samples under a vacuum at 373 K for 15 min to eliminate the adsorbed water. The thermogravimetric analyses were carried out in a TGA 2050 by TA Instruments, under an air flow and with a heating rate of 10 K min^{-1}. The surface acidity was determined after pyridine adsorption by using a FT-IR Perkin-Elmer 1750 spectrometer. At first, a self-supporting wafer of pure catalyst powder was evacuated at 673 K and 10^{-4} Pa; then the adsorption of pyridine was carried out at 303 K by recording the FT-IR spectra

Fig. 2. XRD pattern of the samples: (A) Al–Sn-MCM-41 (CAT L); (B) Ti-MCM-41 (CAT C); (C) Sn-MCM-41 (CAT E); (D) Zr-MCM-41 (CAT G).

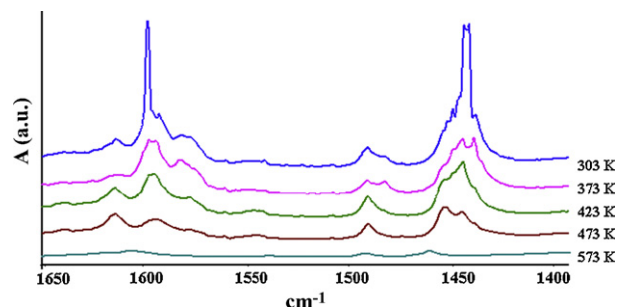following some outgassing steps carried out at different temperatures.

2.4. Catalytic tests

Catalytic tests [temperature = 543–703 K; liquid hourly space velocity (LHSV) = 2.0 h^{-1}; gas hourly space velocity (GHSV) (if not differently reported) = 510 h^{-1}; DHB/formaldehyde acetal = 1:1 mol/mol] were carried out in a fixed-bed glass micro-reactor (i.d. 7 mm, length 400 mm) placed in an electronically controlled oven operating at atmospheric pressure and using 2 cm^3 of pelletized catalyst (40–60 mesh). The isothermal axial temperature profile of the catalytic bed during the tests was controlled by a 0.5 mm J-type thermocouple sliding in a glass capillary tube. Before the tests, the catalyst was maintained at the desired temperature under N$_2$ flow for 1 h. The mixture of DHB and an alkylating agent was fed into the top of the reactor by means of a Precidor model 5003 infusion pump. The products were condensed at 273 K, and analysed using a Carlo Erba 4300 gas chromatograph, equipped with FID and a wide-bore OV1 column (length 30 m, i.d. 0.53 mm, film width 0.5 μm), and tentatively identified by GC–MS with a Hewlett-Packard GCD 1800 system equipped with a HP5 column (length 25 m, i.d. 0.25 mm, film width 1.5 μm). These identifications were subsequently confirmed by comparing the experimental GC–MS patterns with those obtained for reference compounds.

3. Results and discussion

3.1. Catalyst characterisation

XRD powder patterns and FT-IR spectra confirmed that pure MFI-type Ti-silicalite (TS-1) was obtained [26–31,49], with a sur-

Fig. 3. FT-IR spectra of pyridine adsorbed on the sample Sn-MCM-41 (CAT E) (SnO$_2$ = 9.0 wt.%), after outgassing at different temperatures.

face area of 530 m^2 g^{-1}. The XRD powder patterns of MCM-41 doped by heteroatoms were of excellent quality, with typical low angle very strong peak at lower 2θ values and weaker peaks at higher 2θ values, corresponding to the planes 1 0 0, 1 1 0 and 2 0 0, respectively (Fig. 2) [41,49,50]. In addition, the Al-MCM-41 sample with the highest Al-content shows a well-resolved pattern, indicating that a highly ordered mesoporous sample was formed; furthermore, the incorporation of Al^{3+} ions resulted in a shift of the main peak to higher 2θ values for all the samples investigated.
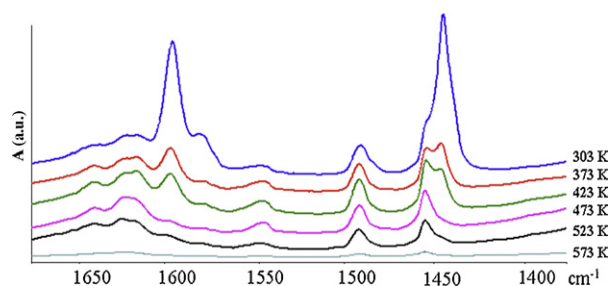
Composition and main data of the samples investigated are reported in Table 1. No significant changes in the physical properties may be observed as a function of the introduction of small amounts of heteroatoms (CAT B–H) in the Si-MCM-41 framework (CAT A). The samples doped with both Al and Ti (or Zr or Sn) (CAT I, L and M) have similar physical properties to the analogous samples which had been prepared without Al (CAT C, E and G).

FT-IR spectra of the catalysts after pyridine chemisorption and subsequent evacuation at different temperatures are a useful tool to determine the amount and strength of surface Lewis- and Brönsted-acid sites [51–53]. All the samples investigated show bands corresponding to hydrogen-bonded pyridine at 1447 and 1599 cm^{-1} [54–61], the only bands observed for the Si-MCM-41 sample (CAT A); for the latter sample the bands completely disappear at 473 K, which indicates that the interaction of pyridine on the sample is weak, due to low acid strength.

The Sn-containing MCM-41 catalysts (Fig. 3) show a band at 1608 cm^{-1} which is attributable to pyridine coordinated on Lewis-acid sites [54–61]. These sites increase proportionally to the number of cations (Sn^{4+} or Ti^{4+}, not reported here) incorporated in the MCM-41 framework. The band at 1450 cm^{-1} can be attributed to a Lewis-type adduct [57]. A slight band at 1577 cm^{-1}, due to pyridine coordinated on weak surface Lewis-acid sites, is also observed for all the Ti- and Sn-MCM-41 samples [55]. In addition, a band corresponding to the vibration of pyridine associated to both Lewis- and Brönsted-acid sites is observed at 1490 cm^{-1}.

Table 1
Molar ratios and chemical–physical properties of the investigated samples.

Sample	Si/Al (mol/mol)	Si/heteroatom (mol/mol)	Pore volume (cm^3 g^{-1})	Average pore size (Å)	Surface area (m^2 g^{-1})
CAT A Si-MCM-41	∞	∞	0.86	34	850
CAT B Ti-MCM-41	∞	50	0.77	39	683
CAT C Ti-MCM-41	∞	20	0.79	35	857
CAT D Sn-MCM-41	∞	50	0.60	34	750
CAT E Sn-MCM-41	∞	20	0.64	32	775
CAT F Zr-MCM-41	∞	50	0.70	36	790
CAT G Zr-MCM-41	∞	20	0.74	38	768
CAT H Al-MCM-41	25	∞	0.51	58	922
CAT I Al–Ti-MCM-41	50	20	0.70	45	790
CAT L Al–Sn-MCM-41	50	35	0.61	38	695
CAT M Al–Zr-MCM-41	50	20	0.69	39	840
TS-1	∞	20	0.53	6	530

Fig. 4. FT-IR spectra of the Al–Sn-MCM-41 sample (CAT L), after outgassing at different temperatures.

Table 2
Lewis [L] and Brønsted [B] acid-site concentration in the samples investigated. The concentration was estimated by pyridine desorption at 373 K under vacuum [44,45].

Sample	[L] (μmol g cat^{-1})	[B] (μmol g cat^{-1})
CAT A Si-MCM-41	0	0
CAT B Ti-MCM-41	146	0
CAT C Ti-MCM-41	390	0
CAT D Sn-MCM-41	152	0
CAT E Sn-MCM-41	440	0
CAT F Zr-MCM-41	289	0
CAT G Zr-MCM-41	n.d.	n.d.
CAT H Al-MCM-41	0	130
CAT I Al-Ti-MCM-41	278	37
CAT L Al–Sn-MCM-41	273	34
CAT M Al–Zr-MCM-41	131	29
TS-1	410	0

Fig. 4 shows a set of *in situ* FT-IR spectra of the sample Al–Sn-MCM-41 (Al_2O_3 = 1.7 wt.%, SnO_2 = 5.0 wt.%) (CAT L) recorded following the adsorption of pyridine and subsequent evacuation at different temperatures. The acidity of Al-containing MCM-41 samples depends directly on the amount of Al present [55,58–61]. In addition to Lewis-acid sites, which are the same as previously observed for the sample CAT E (Fig. 3), the presence of Brønsted-acid sites is shown by the presence of a band at 1545 cm^{-1}. The FT-IR spectra of pyridine adsorbed on the sample TS-1 with Si/Ti = 20 (not reported here) in line with data published [62], show the absence of Brønsted-acid sites, while the amount of Lewis-acid sites is similar to that of the Sn-MCM-41 sample CAT E (Table 2) [52,53].

For the undoped sample Si-MCM-41, the surface acidity could not be valued due to the absence of the referring bands (1545 cm^{-1} for Brønsted- and 1455 cm^{-1} for Lewis-acid sites). In fact, for this sample the only bands detected are those relating to hydrogen-bonded pyridine. Brønsted acidity was therefore generated by the introduction of Al inside the MCM-41 framework, while Lewis-acid sites were derived from the coordination of pyridine with heteroatoms such as Ti, Sn and Zr [62–67]. The Lewis acidity of TS-1 results is higher than in the samples Ti-MCM-41 with the same Si/Ti molar ratio (CAT C).

3.2. Catalytic activity of TS-1

In a preliminary catalytic test, performed at 603 K by feeding an equimolar mixture of DHB/TOX, a higher yield value was obtained than that previously reported [24] (34.5% versus 28.0%, referring to TOX), in spite of the lower amount of alkylating agent present, thus demonstrating the excellent activity of the TS-1 catalyst prepared. Therefore, equimolar mixtures of DHB/alkylating agent were fed in the following tests, in order to avoid recycling costs. All the formaldehyde acetals investigated showed maximum yield and selectivity values in the range of 603–623 K, while the C-balance values are usually higher than 90% in this temperature range.

Regardless of the temperature, poor activity was observed by feeding DMM (conversion $\leq 17.0\%$ and selectivity in MDB $\leq 50\%$), together with the formation of 3-MC and, mainly, 2-MMP, which may be considered as a reaction intermediate (see Section 4). Significantly higher yield and selectivity values were obtained by feeding DEM (Table 3), with an optimum temperature at 623 K, and C-balance values higher than 90%. However, at temperatures higher than 663 K, TS-1 shows significant deactivation, due to the deposition of heavy by-products (tar), as shown by a dramatic decrease in the C-balance. Moreover, the amount of the by-product 3-MC formed is much lower than that observed feeding DMM, whereas no appreciable amount of ethylcatechol is detected.

By increasing the length of the aliphatic chain of the formaldehyde acetal (i.e. feeding DPM), an increase in activity is achieved, although this also produces a loss of selectivity due to significant side reactions (Table 4). It is apparent that DPM is the most active reagent, although the selectivity in MDB is lower than 50%, with the formation of significant amounts of 3-MC and propoxy-phenol, due to the etherification reaction of the n-propanol formed in the synthesis of MDB (Fig. 1) with DHB and, consequently, a worse selectivity in the wanted product. Finally, by feeding DOX (i.e. a cyclic acetal of formaldehyde), surprisingly low yield values in MDB were obtained regardless of the temperature investigated, with significantly high amounts of by-products formed.

Previously [68], some of us demonstrated the very low thermal stability of DMM, which decomposed significantly to formaldehyde and methanol already at temperatures ≤ 603 K, thus resulting not available during catalytic tests. On the contrary, DEM exhibited better thermal stability in the temperature range investigated and, consequently, was more available in catalytic tests, increasing the yield values in MDB (Table 3). Lastly, the very poor catalytic activity observed when feeding DOX may be attributed to its very high stability in the reaction conditions investigated, in which only 10% ca. decomposed to form formaldehyde and glycol, the latter being partially dehydrated to form acetaldehyde and water. It cannot be ruled out, however, that – due to its steric hindrance – DOX may not be capable of interacting properly with DHB.

Table 3
Activity as a function of temperature for the catalyst TS-1 in the synthesis of 1,2-methylenedioxybenzene (MDB), by a reaction of 1,2-dihydroxybenzene (DHB) and diethoxymethane (DEM).

Reaction temperature (K)	DHB convers. (%)	Yield[a] (%)			MDB selectivity[a] (%)
		MDB	2-EMP	3-MC	
543	3.9	0.0	3.5	0.0	0.0
573	8.4	1.1	6.9	0.0	13.1
603	10.3	7.7	2.1	0.0	74.7
623	21.2	18.1	1.2	0.0	85.4
643	25.0	17.5	2.1	0.0	70.0
663	11.4	6.3	3.4	<0.1	55.3
683	4.1	2.1	0.7	0.2	51.2
703	5.7	1.4	0.9	0.8	24.5

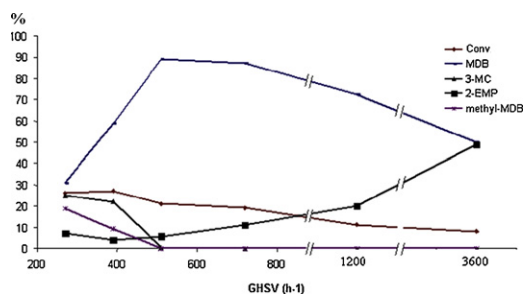[a] Yield and selectivity values referred to DHB.

Table 4

Activity as a function of temperature for the catalyst TS-1 in the synthesis of 1,2-methylenedioxybenzene (MDB) by a reaction of 1,2-dihydroxybenzene (DHB) and dipropoxymethane (DPM).

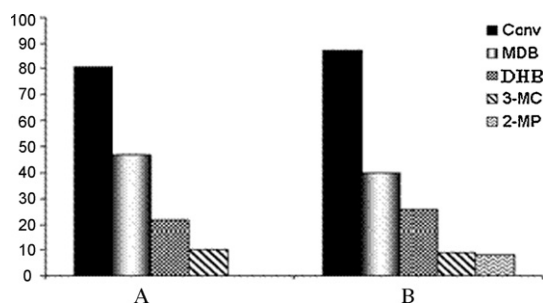| Reaction temperature (K)	DHB convers. (%)	Yield[a] (%)				MDB selectivity[a] (%)
		MDB	2-(Propoxy methoxy) phenol	3-MC	Propoxy-phenol	
603	28.2	11.7	6.1	5.1	4.1	40.0
623	32.7	15.0	4.9	7.0	4.6	45.9

[a] Yield and selectivity values referred to DHB.

Fig. 5. 1,2-Dihydroxybenzene (DHB) conversion and selectivity as a function of GHSV values at 623 K for TS-1 in the synthesis of 1,2-methylenedioxybenzene (MDB) by a reaction of DHB and diethoxymethane (DEM) (*yield and selectivity values referred to DHB).

3.3. Role of the reaction parameters

On the basis of the previous results, the study of the role of reaction parameters was performed using TS-1 and by feeding DHB and DEM, for which the best activity was observed at about 623 K as reported above. Maximum yield and selectivity in MDB values were observed for a GHSV value of 510 h^{-1} (Fig. 5), while increasing values give rise to a progressive decrease in the conversion,
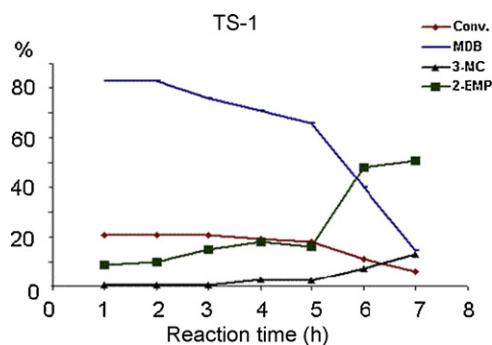

Fig. 6. Reactivity of 2-(ethoxymethoxy)phenol (2-EMP) at 623 K on TS-1 in absence of water (A) or in presence of 10% water (B) (*yield and selectivity referred to 2-EMP).

Fig. 7. 1,2-Dihydroxybenzene (DHB) conversion and product selectivities with time-on-stream at 623 K for TS-1 catalyst in the synthesis of 1,2-methylenedioxybenzene (MDB) by a reaction of DHB and diethoxymethane (DEM) (*conversion and selectivity values referred to DHB).

although the selectivity remains relatively high and the C-balance values are >90%. On the other hand, by decreasing the GHSV values, the selectivity decreases dramatically, due to the C-alkylation side reaction on the aromatic ring, with formation of relevant amounts of 3-MC and a not-fully identified methyl-MDB derivative. Lastly,

Fig. 8. 1,2-Dihydroxybenzene (DHB) conversion and product selectivities with time-on-stream at 623 K for Sn-MCM-41 (CAT E) catalyst in the synthesis of 1,2-methylenedioxybenzene (MDB) by a reaction of DHB and diethoxymethane (DEM) (*conversion and selectivity values referred to DHB).

Table 5

Activity at 623 K for the MCM-41 and TS-1 catalysts in the synthesis of 1,2-methylenedioxybenzene (MDB) by a reaction of 1,2-dihydroxybenzene (DHB) and diethoxymethane (DEM).
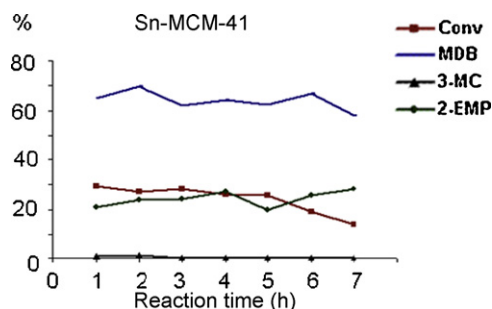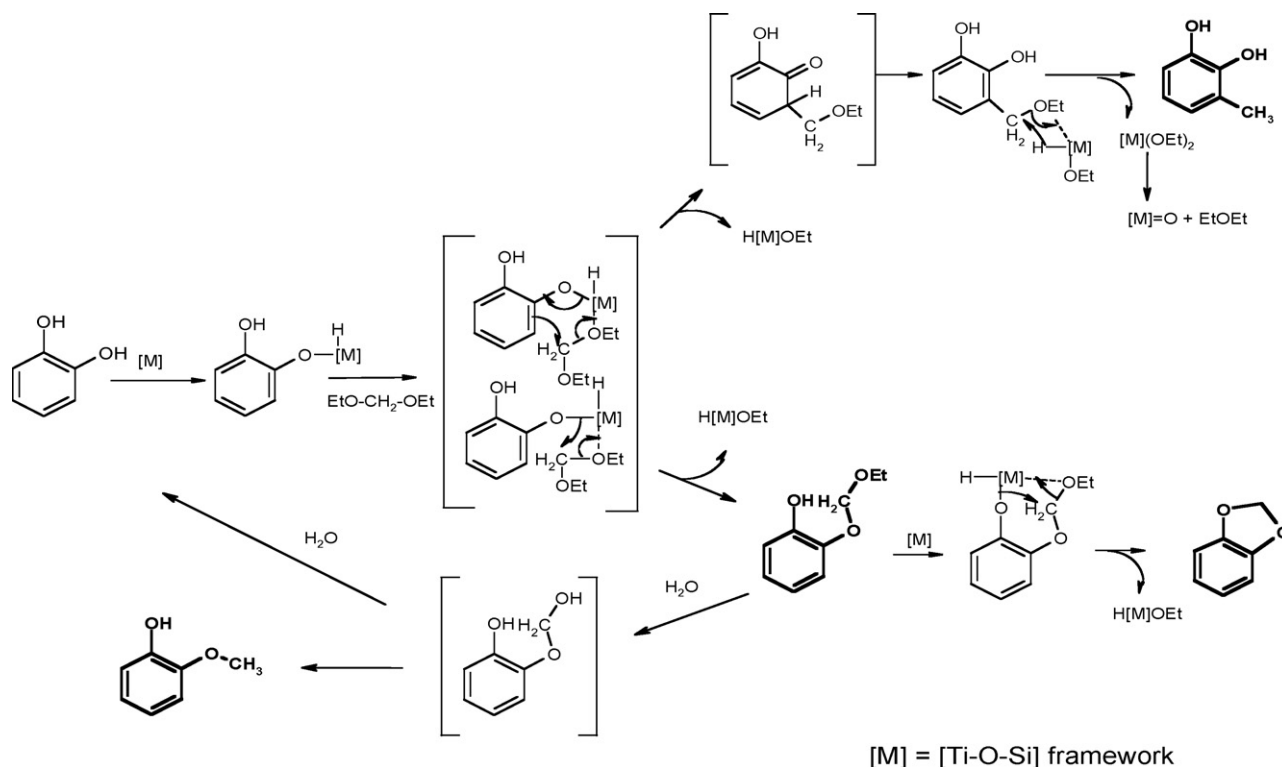
Sample	DHB convers. (%)	Yield[a] (%)			MDB selectivity[a] (%)
		MDB	2-EMP	3-MC	
CAT A Si-MCM-41	14.1	2.0	11.9	–	14.2
CAT B Ti-MCM-41	15.1	7.1	6.7	–	47.0
C AT C Ti-MCM-41	26.9	14.1	10.3	–	52.4
CAT D Sn-MCM-41	15.9	2.1	13.3	–	13.2
CAT E Sn-MCM-41	29.3	19.0	6.1	0.2	64.8
CAT F Zr-MCM-41	18.1	10.9	6.7	–	60.2
CAT G Zr-MCM-41	n.d.	n.d.	n.d.	n.d.	n.d.
CAT H Al-MCM-41	16.6	5.6	7.1	2.9	33.7
CAT I Al–Ti-MCM-41	27.5	11.9	9.7	3.7	43.3
CAT L Al–Sn-MCM-41	33.4	16.4	9.3	3.4	49.0
CAT M Al–Zr-MCM-41	25.0	8.0	11.7	3.8	32.0
TS-1	21.0	18.7	1.2	0.1	89.0

[a] Yield and selectivity values referred to DHB.

Fig. 9. Proposed reaction pathway in the synthesis of 1,2-methylenedioxybenzene (MDB) by reaction of 1,2-dihydroxybenzene (DHB) and diethoxymethane (DEM) [60].

the lowest GHSV value gives rise to the self-condensation of DHB, with the formation of heavy by-products, a dramatic decrease in the C-balance value, and a fast catalyst deactivation.

It has previously been reported that small percentages of water in the feed may improve the catalyst stability with time-on-stream, reducing the formation of tar [69]. In the present reaction, however, the presence of water negatively affects catalytic performances, while reducing in particular the selectivity in MDB (Fig. 6). In the presence of water, the formation of a new by-product is detected, 2-methoxyphenol (2-MP) which is probably derived from the hydrolysis of a reaction intermediate, while no improvement in the C-balance values is observed.

3.4. Catalytic activity of doped MCM-41

Considering the patent constrains on the application of TS-1, the synthesis of MDB from DHB and DEM was investigated using some MCM-41-type catalysts (Table 5). The undoped sample CAT A only promotes the first reaction step, with the formation of mainly 2-EMP and a selectivity in MDB lower than 15%. The introduction of heteroatoms such as Ti, Sn or Zr in the MCM-41 framework favours the formation of Lewis-acid sites and, consequently, increases the cyclization of the reaction intermediate (2-EMP) to MDB. Catalysts with the highest Si/heteroatom ratio (50 mol/mol) exhibit reactivities comparable to those of the undoped sample, indicating that the amount of heteroatom present is not sufficient to significantly modify the catalytic activity, in spite of the textural changes observed. On the other hand, with the lowest Si/heteroatom ratio (20 mol/mol), relevant increases in the conversion values are observed and the selectivity values rise to 60%. In particular, it is worth noting the very good activity of CAT E, containing 9 wt.% of SnO$_2$ in the MCM-41 framework, with a yield in MDB similar to that of TS-1 – although with a lower selectivity value – due to a greater formation of the reaction intermediate 2-EMP.

It is worth noting the almost complete absence of 3-MC for all the Al-free catalysts, which may be correlated to the absence of Brønsted-acid sites, according to what has been previously reported (Fig. 4). The presence of 3-MC suggests that the side C-alkylation reaction is favoured by the presence of Brønsted-acid sites, since the formation of 3-MC was not detected for Al-free samples. Finally, it is evident that the presence of Al mainly worsens the selectivity, while the conversion values are almost the same for all the samples, regardless of Al-presence.

3.5. Catalyst stability and regeneration

Together with the catalytic activity, the catalyst stability and its possible regeneration are also important parameters, which were investigated for the two samples with the best performances, i.e. TS-1 and CAT E. After 5 h of time-on-stream, the TS-1 catalyst shows a significant decrease in activity (Fig. 7), mainly related to the formation of heavy by-products (tar) by DHB self-condensation on the surface [70,71]. The Sn-MCM-41 sample (CAT E) exhibits similar behaviour (Fig. 8), although its deactivation results are slower than that observed for TS-1 Furthermore, the selectivity in MDB decreases significantly with time-on-stream for TS-1, while for CAT E it remains more or less constant regardless of the value of the reaction time.

The causes of deactivation may be investigated by thermogravimetric analysis (TGA) carried out in air on the catalyst after long-time tests. TGA profiles show the presence of two weight losses: the first one, at 523 K ca., may be attributed to the desorption of reagents and/or products adsorbed on the surface, while the second one, at 743 K ca., is attributable to the combustion of the heavy by-products deriving from the DHB self-condensation, which is the main cause of the deactivation. On the basis of these results, the catalysts were calcined at 773 K for 6 h. Regenerated catalysts show slight decreases in their surface area: 450 m^2 g^{-1} versus 530 m^2 g^{-1} for TS-1 and 680 m^2 g^{-1} versus 775 m^2 g^{-1} for CAT E. Both catalysts

recovered their initial activity almost completely, although proving to be less stable with time-on-stream than fresh catalysts.

4. Possible reaction pathway

2-EMP was previously suggested to be the key reaction intermediate. It was confirmed when feeding 2-EMP, as such or together with water. As expected, MDB was formed up to 47.0%, together with a smaller amount of 3-MC, thus evidencing that 2-EMP may be the intermediate for both reaction products. It is worth noting co-feeding water also the formation of significant amounts of DHB, as it shows that the reaction of DHB and DEM to produce 2-EMP is reversible. The presence of water not only increased the amount of DHB, but also favoured the formation of 2-MP. On the other hand, the formation of another by-product, 3-MC, was favoured by Brønsted-acid sites. On the basis of the reported data, a possible reaction pathway may be proposed (Fig. 9).

5. Conclusions

An environmentally friendly synthesis of MDB can be efficiently carried out in the vapour phase, by feeding DHB and formaldehyde acetals in a 1:1 molar ratio and using a catalyst containing weak acid sites and redox sites. Among the different formaldehyde acetals, the best values were obtained by feeding DEM and operating in the temperature range of 603–643 K and for a GHSV value of $510 \, h^{-1}$. TS-1 and a Sn-MCM-41 (Si/Sn = 20 mol/mol) were the most active and selective catalysts, thus evidencing the role of well-dispersed tetrahedrally coordinated Ti^{4+} or Sn^{4+} ions. The Sn-containing sample showed a slower deactivation than TS-1, while maintaining a suitable activity for 6–7 h ca. Catalysts deactivated mainly because of the deposition of heavy by-products by DHB self-condensation; however, the initial catalytic activity can be partially recovered by calcination at 773 K for 6 h.

Acknowledgements

References

[1] V. Borzatta, C. Gobbi, E. Capparella, E. Poluzzi, WO Patent 042,512 (2005) to Endura.
[2] K.G. Fahlbusch, F.J. Hammerschmidt, J. Panten, W. Pickenhagen, D. Schatkowski, K. Bauer, D. Garbe, H. Surburg, in: B. Elvers, M. Bohmet, S. Hawking, W.E. Russey (Eds.), Ullmann's Encyclopedia of Industrial Chemistry, vol. 14, 6th ed., Wiley–VCH, Wenheim, 2003, p. 73.
[3] M. Zively, in: J.I. Kroschwitz (Ed.), Kirk–Othmer Encyclopedia of Chemical Technology, vol. 3, 5th ed., Wiley, New York, USA, 2007, p. 226.
[4] M. Kushiro, T. Masaoka, S. Hageshita, Y. Takahashi, T. Ide, M. Sugano, J. Nutr. Biochem. 13 (2002) 289.
[5] http://www.erowid.org.
[6] G. Salmoria, E. Dall'Oglio, C. Zucco, Synth. Commun. 27 (1997) 4335.
[7] P. Vanelle, J. Meuche, J. Maldonado, M.P. Crozet, F. Delmas, P. Timon-David, Eur. J. Med. Chem. 35 (2000) 157.
[8] Flavors and Fragrances of Plant Origin, FAO Report M37, 1995.
[9] M. Shirai, Y. Yoshida, S. Sadaike, WO Patent 054,997 (2004) to Ube Industries.
[10] P. Maggioni, US Patent 4,183,861 (1980) to Brichima.
[11] J.W. Cornforth, US Patent 3,436,403 (1969) to Shell Oil.
[12] J.A Kirby, US Patent 4,082,774 (1978) to Eli Lilly.
[13] P. Panzeri, G. Castelli, V. Messori, Eur. Patent 0,877,023 (1998) to Borregaard Italia.
[14] V. Borzatta, D. Pantaleoni, US Patent 6,342,613 (2002) to Endura.
[15] B. Jursic, Tetrahedron 44 (1988) 6677.
[16] J.H. Clark, H.L. Holland, J.M. Miller, Tetrahedr. Lett. 17 (1976) 3361.
[17] S. Porchet, L. Kiwi-Minsker, R. Doepper, A. Renken, Chem. Eng. Sci. 51 (1996) 2933.
[18] L. Kiwi-Minsker, S. Porchet, R. Doepper, A. Renken, Stud. Surf. Sci. Catal. 108 (1997) 149.
[19] L. Calzolari, F. Cavani, T. Monti, Compte Rend. Acad. Sci., Series IIc: Chem. 3 (2000) 533.
[20] F. Cavani, T. Monti, D. Paoli, Stud. Surf. Sci. Catal. 130C (2000) 2633.
[21] V. Vishwanathan, S. Ndou, L. Sikhwivhilu, N. Plint, K.V. Raghavan, N.J. Coville, Chem. Commun. (2001) 893.
[22] X. Zhu, X. Lia, M. Jia, G. Liu, W. Zhang, D. Jiang, Appl. Catal. A 282 (2005) 155.
[23] F. Luque, J.M. Campelo, T.D. Conesa, D. Luna, J.M. Marinas, A.A. Romero, New J. Chem. 30 (2006) 1228.
[24] J. Roland, J. Desmurs, WO Patent 108,385 (2005) to Rhodia Chimie.
[25] M. Ardizzi, N. Ballarini, F. Cavani, E. Chiappini, L. Dal Pozzo, L. Maselli, T. Monti, Appl. Catal. B 70 (2007) 597.
[26] M. Taramasso, G. Perego, B. Notari, US Patent 4,410,501 (1983) to Enichem.
[27] U. Bellussi, A. Esposito, M. Clerici, U. Romano, US Patent 4,701,428 (1987) to Enichem Sintesi.
[28] X. Wang, X. Guo, Catal. Today 51 (1999) 177.
[29] J.P. Catinat, M. Stebelle, US Patent 6,169,050 (2001) to Solvay.
[30] T. Yokoi, P. Wu, T. Tatsumi, Catal. Commun. 4 (2003) 11.
[31] H. Liu, G. Lu, Y. Guo, Appl. Catal. A 293 (2005) 153.
[32] P. Selvam, S.E. Dapurkar, Catal. Today 96 (2004) 135.
[33] A. Vinu, M. Karthik, M. Miyahara, V. Murugesan, K. Ariga, J. Mol. Catal. A: Chem. 230 (2005) 151.
[34] J. Huang, L. Xing, H. Wang, G. Li, S. Wu, T. Wu, Q. Kan, J. Mol. Catal. A: Chem. 259 (2006) 84.
[35] K. Shanmugapriya, M. Palanichamy, V.V. Balasubramanian, V. Murugesan, Micropor. Mesopor. Mater. 95 (2006) 272.
[36] K. Rajasekar, A. Pandurangan, Catal. Commun. 8 (2007) 635.
[37] R. Luque, J.M. Campelo, D. Luna, J.M. Marinas, A.A. Romero, J. Mol. Catal. A: Chem. 269 (2007) 190.
[38] D. Zhao, J. Zhao, S. Zhao, Prog. Chem. 19 (2007) 510.
[39] B. Ràc, M. Nagy, I. Pàlinkò, A. Molnàr, Appl. Catal. A 316 (2007) 152.
[40] A. Corma, Chem. Rev. 97 (1997) 2373.
[41] S. Biz, M.L. Occelli, Catal. Rev. Sci. Eng. 40 (1998) 329.
[42] A. Taguchi, F. Schüth, Micropor. Mesopor. Mater. 77 (2005) 1.
[43] A. Corma, M.T. Navarro, L. Nemeth, M. Renz, Chem. Commun. (2001) 2190.
[44] K.A. Koyano, T. Tatsumi, Micropor. Mater. 10 (1997) 259.
[45] S. Gontier, A. Tuel, Zeolites 15 (1995) 601.
[46] A. Corma, J.L. Jorda, M.T. Navarro, R. Rey, Chem. Commun. (1998) 1899.
[47] T. Blasco, A. Corma, M.T. Navarro, J. Perez Pariente, J. Catal. 156 (1995) 65.
[48] A. Corma, L.T. Nemeth, M. Renz, S. Valencia, Nature 412 (2001) 423.
[49] http://www.iza-structure.org.
[50] F. Hoffmann, M. Cornelius, J. Morell, M. Fröba, Angew. Chem., Int. Ed. 45 (2006) 3216.
[51] J.S. Beck, J.C. Vartuli, W.J. Ruth, M.E. Leonowicz, C.T. Kresge, K.D. Schmitt, C.T.-W. Chu, D.H. Olson, E.W. Sheppard, S.B. Higgins, J.B. Higgins, J.L. Schlenker, J. Am. Chem. Soc. 114 (1992) 10834.
[52] J. Datka, A.M. Turek, J.M. Jehng, I.E. Wachs, J. Catal. 135 (1992) 186.
[53] Z. Luan, C. Cheng, W. Zhou, J. Klinowski, J. Phys. Chem. 99 (1995) 1018.
[54] E.P. Parry, J. Catal. 2 (1963) 371.
[55] C.A. Emeis, J. Catal. 141 (1993) 347.
[56] B. Chakraborty, B. Viswanathan, Catal. Today 49 (1999) 253.
[57] D. Trong On, S. Nguyen, V. Hulea, E. Dumitriu, S. Kaliaguine, Micropor. Mesopor. Mater. 57 (2003) 169.
[58] A. Sakthivel, S. Dapurkar, N. Gupta, S. Kulshreshtha, P. Selvam, Micropor. Mesopor. Mater. 65 (2003) 177.
[59] D. Srinivas, R. Srivastava, P. Ratnasamy, Catal. Today 96 (2004) 127.
[60] T. Conesa, J. Hidalgo, R. Luque, J. Campelo, A. Romero, Appl. Catal. A 299 (2006) 224.
[61] M.A. Zanjanchi, M. Vaziri, Mater. Chem. Phys. 110 (2008) 61.
[62] H. Kosslick, G. Lischke, G. Walther, W. Storek, A. Martin, R. Fricke, Micropor. Mater. 9 (1997) 13.
[63] L. Cedeno, D. Hernandez, T. Klimova, J. Ramirez, Appl. Catal. A 241 (2003) 39.
[64] C. Otero Arean, M. Rodriguez Delgado, V. Montouillout, J. Lavalley, C. Fernandez, J. Cuart Pascual, J. Parra, Micropor. Mesopor. Mater. 67 (2004) 259.
[65] G. Turnes Palomino, J. Cuart Pascual, M. Rodrıguez Delgado, J. Bernardo Parra, C. Otero Arean, Mater. Chem. Phys. 85 (2004) 145.
[66] A. Infantes-Molina, J. Merida-Robles, P. Maireles-Torres, E. Finocchio, G. Busca, E. Rodriguez-Castellon, J.L.G. Fierro, A. Jimenez-Lopez, Micropor. Mesopor. Mater. 75 (2004) 23.
[67] L. Chen, L. Norenã, J. Navarrete, J. Wang, Mater. Chem. Phys. 97 (2006) 236.
[68] D. Impalà, O. Piccolo, A. Vaccari, in: M.L. Prunier (Ed.), Catalysis of Organic Reactions, CRC, Boca Raton, FL, 2009, p. 345.
[69] E.M. Miller, US Patent 4,001,282 (1977) to General Electric.
[70] S. Sanchez-Cortes, O. Francioso, J.V. Garcıa-Ramos, C. Ciavatta, C. Gessa, Colloids Surf. A: Physicochem. Eng. Aspects 176 (2001) 177.
[71] D.F. McMillen, R. Malhotra, S. Chang, S.E. Nigenda, Fuel 83 (2004) 1455.